Published in final edited form as:
Auton Neurosci. 2010 December 8; 158(1-2): 13–23. doi:10.1016/j.autneu.2010.05.006.

An arcuate-ventrolateral periaqueductal gray reciprocal circuit participates in electroacupuncture cardiovascular inhibition

Peng Li[*], **Stephanie C. Tjen-A-Looi**, **Zhi-Ling Guo**, and **John C. Longhurst**
Department of Medicine, Susan-Samueli Center for Integrative Medicine, School of Medicine, University of California, Irvine CA 92697-4075, United States

Abstract

Electroacupuncture (EA) suppresses elevated blood pressure (BP) by activating the arcuate nucleus, ventrolateral periaqueductal gray (vlPAG), and inhibiting cardiovascular sympathetic neurons in the rostral ventrolateral medulla. This study investigated the reciprocal neural circuit between arcuate and vlPAG during EA inhibition of reflex increases in blood pressure. In α-chloralose anesthetized cats the gallbladder or splanchnic nerve was stimulated to induce cardiovascular sympathoexcitatory reflexes. Electrophysiological recordings showed that EA facilitates the arcuate neural response to splanchnic nerve stimulation. Bilateral vlPAG microinjection of D,L-homocysteic acid (DLH) facilitated the arcuate response to splanchnic nerve stimulation, while microinjection of kainic acid blocked EA (P 5–6 acupoints on pericardial meridian, overlying the median nerves) excitation of arcuate neurons. Retrograde microsphere tracer labeling in the arcuate or vlPAG perikarya was found after respective microinjection of the tracer in the vlPAG or arcuate of rats, demonstrating reciprocal direct connections between the two nuclei. EA inhibition of reflex-induced BP elevation was blocked by injection of glutamate or cholinergic receptor antagonist, kynurenic acid or atropine, into the arcuate. Excitation of vlPAG neurons during EA was blocked by arcuate microinjection of glutamate NMDA and non-NMDA receptor antagonists, AP-5 and CNQX, or the cholinergic receptor antagonist, atropine. Microinjection of DLH or acetylcholine (ACh) into the arcuate facilitated EA excitation of vlPAG neurons. Microinjection of AP5 and CNQX, but not atropine, into the vlPAG blocked EA excitation of arcuate neurons. Thus, a reciprocal excitatory glutamatergic neural circuit between the arcuate and vlPAG contributes to long-lasting EA cardiovascular inhibition. ACh in the arcuate but not in the vlPAG participates in the reciprocal excitation.

Keywords

Glutamatergic receptors; Acetylcholine; Kainic acid; Kynurenic acid; Retrograde tracer

1. Introduction

Cardiovascular disease is the major cause of death in North America, Europe and China. There has been increasing interest in the western countries in exploring new medical treatments such as acupuncture for cardiovascular diseases. A number of small clinical reports suggest that acupuncture can reduce blood pressure (BP) in hypertensive patients (Tam and Yiu, 1975; Zhang, 1956). In this regard, a recent preliminary study from our laboratory has shown that electroacupuncture (EA) applied once weekly at a combination of acupoints for 6–8 weeks in patients with mild to moderate hypertension reduces BP for more

[*]Corresponding author. Medical Science I, C250, School of Medicine, University of California, Irvine CA 92697-4075, United States. Tel.: +1 949 824 6123; fax: +1 949 824 2200. pengli@uci.edu (P. Li).

than a month following cessation of the acupuncture therapy (Li and Longhurst, 2007). Furthermore, in animal experimental studies, we have shown that EA inhibits BP elevations induced by application of bradykinin to the gallbladder to mimic cholecystitis (Li et al., 1998). Thirty minutes of EA decreases the elevation in blood pressure associated with sympathetic cardiovascular reflex activation frequently for more than 70 min (Tjen-A-Looi et al., 2007). EA inhibits the neuronal response in the rostral ventrolateral medulla (rVLM) for about 1 h (Tjen-A-Looi et al., 2003), suppresses the cardiovascular responses in anesthetized animals for 1 to 6 h (Guo et al., 1981; Lovick et al., 1995) and inhibits elevated blood pressure of conscious animals with spontaneous hypertension for as long as 1 to 12 h (Lin and Li, 1981; Yao et al., 1982). The pathways and mechanisms contributing to the long-lasting EA inhibitory effect are not understood completely. We have demonstrated that GABA and opioids, but not nociceptin, in the rVLM contribute, in part, to the long-lasting EA inhibition (Tjen-A-Looi et al., 2007). We also have shown that EA inhibition of rVLM premotor sympathetic cardiovascular neurons involves a long-loop pathway in the hypothalamus, midbrain and medulla. In this regard, EA activates the hypothalamic arcuate nucleus and facilitates the arcuate neuronal responses to afferent input during splanchnic nerve stimulation. These arcuate neurons send excitatory projections to the ventrolateral periaqueductal gray (vlPAG) (Li et al., 2006) which, in turn, activates μ and δ-opioid receptors in the rVLM to modulate cardiovascular sympathetic premotor neurons (Li et al., 2001; Tjen-A-Looi et al., 2006). However, although we have shown that the arcuate contributes to EA-related inhibition of cardiovascular sympathoexcitatory reflex responses, the mechanisms underlying the ability of the long-loop pathway, which, as noted above, involve the arcuate as well as the vlPAG (Li et al., 2006, 2009; Tjen-A-Looi et al., 2007) are uncertain.

In our preliminary study, we demonstrated that stimulation of the arcuate activated vlPAG neurons, while stimulation of vlPAG in turn evoked activity in the arcuate nucleus. The present study therefore postulated the existence of reciprocal excitatory projections between the arcuate and vlPAG, which are activated by EA and contribute to prolonged suppression of sympathoexcitatory reflex responses. We further postulated that both glutamate and acetylcholine (ACh) contribute to the reciprocal excitation in both nuclei. A preliminary communication of this study has been published (Li et al., 2008).

2. Methods and materials

2.1. Surgical preparation

The experimental preparations and protocols for this study were reviewed and approved by the Animal Care and Use Committee of the University of California, Irvine CA. The studies conformed to the American Physiological Society guidelines and principles for research involving animals. Adult cats of either sex (2.1–5.8 kg) were anesthetized by injection of ketamine (40 mg/kg S.C.) followed by α-chloralose (50 mg/kg I.V.). Additional injections of α-chloralose (5 mg/kg I.V.) were given to maintain an adequate depth of anesthesia, as assessed by the lack of a response (including pupil dilatation) to noxious toe pinch, a respiratory pattern that followed the ventilator (i.e. not over-breathing) and a stable blood pressure and heart rate. The magnitudes of responses to splanchnic nerve or gallbladder stimulation and EA at P 5–6 acupoints were unchanged by supplemental anesthesia. The trachea was intubated and respiration was maintained artificially (model 66, Harvard Apparatus, South Natick, MA). Gallamine triethiodide (4 mg/kg) was administered intravenously before recording neuronal activity to avoid muscle movement during stimulation of somatic nerves. Following paralysis, supplemental α-chloralose was administered on a regular basis. The magnitudes of responses to splanchnic nerve or gallbladder stimulation and EA at P 5–6 acupoints (P refers to the pericardium meridian along the forelimb, see protocols below) were unchanged by supplemental anesthesia.

Arterial blood gases and pH were measured periodically in all animals with a blood gas analyzer (model ABL3, Radiometer, Copenhagen, Denmark). Arterial PO_2 and PCO_2 were kept within normal limits (CO_2 30–35 mm Hg; PO_2 > 100 mm Hg) by enriching the inspired O_2 supply and adjusting the ventilation rate or volume. Arterial pH was maintained between 7.34 and 7.43 and corrected, as necessary, by administering 8% sodium bicarbonate. Body temperature was monitored with a rectal probe connected to a thermometer (model 44TD, Yellow Springs Instrument, Yellow Springs, OH) and was maintained at a range of 36–38°C by a water-heating pad and a heating lamp.

The left femoral vein was cannulated for administration of drugs and fluids. Systemic arterial blood pressure was monitored by a pressure transducer (model 1290, Hewlett-Packard, Waltham, MA) attached to a cannula inserted into the left femoral artery.

A laparotomy provided exposure of the gallbladder and isolation of the splanchnic nerve. The splanchnic nerve was placed on a bipolar stimulating electrode connected to an isolation unit and a stimulator (Grass, model S88). Expoxy dental glue (Pentron, Willingford, CT) was used to isolate the electrodes and to hold the intact nerve in place. In a few experiments near the end of the experiment, the splanchnic nerve was tied at the distal end. Stimulation of its central part showed the same result as before. The abdominal wall was closed with clips to maintain moisture in the abdominal cavity and to prevent heat loss. It was reopened only when filter paper, dipped in bradykinin (BK, 10 μg/ml), was applied to the serosal surface of the gallbladder. Thereafter, the neural axis of the cat was stabilized with a stereotaxic head frame (Kopf). A dorsal craniotomy was performed to expose the hypothalamic arcuate nucleus and midbrain periaqueductal gray for recording extracellular activity and for bilateral microinjection of agonists, antagonists or vehicle controls.

2.2. Stimulation, recording and microinjection

The splanchnic nerve was stimulated with 0.2–0.4 mA, and 0.5 ms pulses at 2 Hz with a Grass stimulator (Model S88K) at a level sufficient to induce a reflex increase in blood pressure. Electroacupuncture was applied bilaterally using pulses of 1–4 mA, 0.5 ms duration and 2 Hz at the P 5–6 acupoints (pericardium meridian, sometimes designated PC) for 30 min. We have demonstrated previously that EA at these locations (Neiguan and Jianshi, respectively located 1.5–2.0 and 2.5–3.0 cm above the wrist between the ligaments of the flexor carpi radialis and the palmaris longus) stimulates the median nerves that project to the spinal segments between C_8 and T_1 and modulates sympathoexcitatory cardiovascular responses (Li et al., 2001, 2006; Tjen-A-Looi et al., 2007).

Using the atlas of Fikova and Marsala (1967) as a guide, glass pipettes with platinum recording wires were positioned perpendicularly to the cortex (0.7–1.0 mm lateral on either side of the midline, 0–2 mm or 9.5–11.5 mm rostral to the tentorium), then lowered 22 or 28 mm from the dorsal surface of the midbrain or hypothalamus to access the vlPAG and arcuate, respectively. Stainless steel tubes (guide tubes 0.8 mm, injection tubes 0.4 mm in diameter and 1 mm longer than the guide tube) for microinjection were inserted into the arcuate and rostral vlPAG using the same coordinates as the recording electrodes. In some animals, guide tubes were positioned using a 77° angle from the dorsal surface toward the caudal part of the animal, and 2–5 mm anterior to the tentorium to approach the caudal vlPAG, since this region of the vlPAG has been shown to play a role in the arcuate-rVLM long-loop pathway (Li et al., 2008, 2009). The locations of both nuclei were identified preliminarily by microinjecting 50 nl of 4 nM D,L-homocysteic acid (DLH) to evoke small but reproducible transient (1–2 min) decreases in blood pressure of 5 to 10 mm Hg. Single-unit extracellular activity in the arcuate or vlPAG was recorded with a single-barrel glass pipette containing 0.5 M sodium acetate and 2% Chicago sky blue (Sigma Chemical, St Louis, MO). Evoked activities of arcuate and vlPAG neurons were recorded during

stimulation of the splanchnic nerve and P 5–6 acupoints. All the recorded neurons were identified by evoked activities during both the splanchnic nerve and P 5–6 acupoint stimulation, thus documenting that they received visceral and somatic convergent input.

To evaluate the influence of EA on arcuate and vlPAG neuronal activity, action potentials were amplified with a preamplifier (Neuroprobe Amplifier Model 1600, A-M Systems, Inc.) attached to a Nerve Traffic Analysis System 662C-3 (Bioengineering, College of Medicine, University of Iowa), then filtered (3–10 KHz) and monitored with an oscilloscope (Tektronix 2201). Action potentials, blood pressures and heart rates were digitized and analyzed online with a Pentium IV computer and a four-channel data acquisition system (SHMU; Shanghai Medical College of Fudan University, China).

2.3. Chemicals for microinjection

All chemicals are from Sigma-Aldrich (St. Louis, MO). Chemicals were dissolved in normal saline and included DLH (4 nM); kainic acid (KA, 1 mM); glutamatergic antagonist kynurenic acid (KYN, 100 nM); glutamatergic N-methyl-D-aspartate (NMDA) ionotropic receptor antagonist amino-5-phosphonovaleric acid (AP5, 25 mM) (Gee et al., 2002; Zhou et al., 2007) glutamatergic (non-NMDA, AMPA, α-amino-3-hydroxy-5-methyl-4-isoxazolepropionic acid) ionotropic receptor antagonist 6-cyano-7-nitro-quinoxaline-2,3-dione (CNQX, 2 mM); acetylcholine (ACh 11 mM) and muscarinic antagonist atropine (3.5 mM). The volume of microinjections was 50 nl.

2.4. Verification of injection and recording sites

Animals were euthanized with α-chloralose followed by intravenous saturated KCl at the end of each experiment. Recording sites then were marked by microinjection (50 nl) of 2% Chicago blue dye. The hypothalamus, midbrain and medulla were removed and fixed in 10% formalin for 4–7 days. Frozen serial 60 μm brain sections were cut with a freezing microtome (Leica CM 1850). Slices were stained with neutral red and examined with a microscope (Nikon eclipse 6400) to identify recording and microinjection sites. These areas were reconstructed from the dye spots with New Bitmap Image plotted on coronal sections that were separated by 1–2 mm, with respect to the auditory line. Composite coronal caudal and rostral sections were constructed from multiple tissue sections. Sections were scanned and traced with Corel suite software. Nuclei were superimposed with nuclear structures identified with the aid of the atlas of Fikova and Marsala for the hypothalamus and midbrain (Fikova and Marsala, 1967).

3. Experimental protocols

3.1. Characteristics of arcuate and vlPAG neurons

The animal was stabilized after surgery for 1–2 h prior to neural recording. All recorded arcuate and vlPAG neurons were evaluated for their responses to both splanchnic nerve and P 5–6 acupoint stimulation. Only those neurons that responded to both inputs were studied.

3.2. Influence of vlPAG neurons on arcuate response to splanchnic stimulation

In six animals, the arcuate neural responses to repeated splanchnic nerve stimulation were measured every 10 min to determine consistency. In another eight animals, after the splanchnic nerve was stimulated twice, DLH (4 nM, 50 nl) was microinjected bilaterally into the vlPAG to evaluate the influence of vlPAG excitation on the arcuate response to splanchnic nerve stimulation. In five other cats, KA (1 mM, 50 nl) was injected bilaterally into the vlPAG to induce brief depolarization blockade (Li et al., 2006, 2009). As a control, in 11 cats normal saline (NS) was microinjected into the vlPAG to evaluate the EA influence on the arcuate response to splanchnic nerve stimulation.

3.3. Glutamate in reciprocal arcuate-vlPAG projections

3.3.1. Arcuate/vlPAG and vlPAG glutamate—Pressor reflexes were induced by application of bradykinin (BK, 10 μg/ml) on the gallbladder every 10–15 min (Li et al., 1998; Tjen-A-Looi et al., 2006). Then, 30 min of EA at P 5–6 (2–4 mA, 2 Hz) was applied. The glutamate receptor antagonist, kynurenic acid (100 nM) was micro-injected into the arcuate or vlPAG (n=5/7) bilaterally after 30 min of EA to evaluate its influence on EA inhibition of the BK-induced pressor reflex.

3.3.2. Hypothalamic and midbrain glutamate ionotropic receptors in EA vlPAG-arcuate responses—The NMDA and non-NMDA antagonists AP 5 (25 mM, 50 nl, n=5) and CNQX (2 mM, 50 nl, n=7) were microinjected into the arcuate to examine the role of these ionotropic glutamate receptors in EA excitation of the vlPAG neuronal response. In separate animals, AP5 (n=4) and CNQX (n=4) were microinjected into the vlPAG prior to EA to examine the importance of these receptors in EA-related excitation of the arcuate response.

3.4. Cholinergic system in ARC-vlPAG reciprocal projections

In five cats, ACh was microinjected into the arcuate or vlPAG to evaluate its effect on BP. The sympathoexcitatory reflexes were induced by application of BK (10 μg/ml) to the gallbladder every 10–15 min. EA was applied at P 5–6 (4 mA, 2 Hz) for 30 min. The cholinergic muscarinic receptor antagonist, atropine (3.5 mM, 50 nl) was microinjected bilaterally into the arcuate after the BK-induced increase of BP was inhibited by EA to evaluate the role of cholinergic receptor activation during EA inhibition of the BK-induced pressor reflex.

In another group of animals ACh was microinjected bilaterally into arcuate (n=8) or vlPAG (n=5) to evaluate its influence on the vlPAG or arcuate neuronal response to splanchnic nerve stimulation. In other cats atropine was microinjected into arcuate (n=5) or vlPAG (n=5) to test its influence on the splanchnic stimulation-induced neuronal response and EA excitation of vlPAG/arcuate neurons.

3.5. Microinjection of a retrograde tracer into vlPAG and arcuate nuclei

We have shown previously that the anatomical circuitry of the long-loop pathway that participates in the EA cardiovascular inhibitory response in rats is virtually similar to that of cats (Adams, 1979; Li et al., 2009). Thus, following stereotaxic positioning injection pipettes in the vlPAG or arcuate, we microinjected a retrogradely transported microsphere tracer in 350–500 g rats to anatomically examine for direct projections between the arcuate and vlPAG nuclei, using a protocol similar to that used in our previous studies in rats (Li et al., 2009). A mixture of ketamine/xylazine (80/12 mg/ml, Sigma) was used to induce (0.3–0.4 ml, i.m) and maintain (0.1–0.2 ml, i.m) anesthesia in these animals. Body temperature was monitored with a rectal probe and was maintained at 37 °C. Heart rate and oxygen saturation were monitored using a pulse oximeter (Nonin Medical, Inc. Plymouth, MN USA). Following induction, rats were positioned in a stereotaxic apparatus (David Kopf Instruments). A one-inch incision was made to expose the skull. A burr hole (4 mm diameter) was made in the bone so that the pipettes could be inserted using the following coordinates: for vlPAG injection, 7.0–8.8 mm caudal from the bregma; 0.5–1.2 mm from the midline, 6.0–6.8 mm deep from the dural surface; for arcuate injection, 1.8–3.6 mm caudal from the bregma; 0.3–0.5 mm from the midline, 8.8–9.6 mm deep from the dural surface. The retrogradely transported tracer, rhodamine-labeled fluorescent microspheres in suspension (0.04 μm, Molecular Probes, Eugene, OR), was injected unilaterally into the vlPAG or arcuate through a glass micropipette (100 nl). The wound was sutured shut. The microspheres were transported during a 10–12 day recovery and maintenance period.

Terminal procedures occurred 10 to 12 days after administration of the retrograde tracer. Rats were re-anesthetized with ketamine/xylazine, as described above. After tracheotomy and intubation, the cannulation and monitoring of vital signs were similar to the procedures described above for cats. Animals were stabilized for 4 h. They then were anesthetized deeply with a large dose of the ketamine/xylazine (0.5–0.7 ml, i.m.). Transcardial perfusion was performed using 500 ml of 0.9% saline solution followed by 500 ml of 4% paraformaldehyde. The hypothalamus and midbrain were harvested and sliced in coronal sections (30 μm) using a cryostat microtome (Leica CM1850 Heidelberger Strasse, Nussloch, Germany). Neurons labeled with retrograde microsphere tracer in the midbrain or hypothalamus were visualized in 30 μm sections and from the same rat the injected nuclei were visualized in 50 μm slices to identify sites of microsphere tracer injection.

Brain sections were scanned and examined with a standard fluorescent microscope (Nikon, E400, Melville, NY, USA). The epifluorescence filter (G-2A), equipped in a fluorescent microscope, was used to identify the stain, appearing as red (rhodamine) in brain sections. Sections containing neurons labeled with the red retrograde tracer and the regions showing injection site of the tracer in ARC and vlPAG were identified according to the best matched standard stereotaxic plane, as shown in Paxinos and Watson's (2005) atlas for the rat.

After examination with a fluorescent microscope, selected sections containing neurons that were labeled with the retrograde tracer were evaluated further with a laser scanning confocal microscope (Zeiss LSM 510, Meta system, Thornwood, NY, USA). A 543 nm wavelength laser was used to excite rhodamine (red). Digital fluorescent images were captured and analyzed with software (Zeiss LSM) provided with the confocal microscope. Each confocal section analyzed was limited to 0.5 μm thickness in the Z-plane.

4. Statistical analysis

Data are presented as means±SEM. The assumption of normal data distribution was evaluated with the Kolmogorov–Smirnov test. BP and neural activity (imp/30 stimuli) in response to splanchnic nerve stimulation before, during and after EA, and after delivery of saline, DLH, KA, glutamatergic and cholinergic receptor antagonists were assessed using a one-way repeated measures analysis of variance, followed by the Holm–Sidak test post hoc (more power than the Tukey and Bonferroni test as recommended by SigmaStat 3.0). This analysis represents a pair wise multiple comparisons procedure. Data in Tables 1 and 2 were compared using a Student's *t*-test. We utilized SigmaStat and SigmaPlot software (Jandel Scientific, San Rafael, CA) for the statistical analyses and graphing. The 0.05 probability level was used to determine statistically significant differences.

5. Results

5.1. Characteristics of arcuate and vlPAG neurons

We examined 41 arcuate neurons and 28 neurons (68%) that responded to both splanchnic nerve and P 5–6 (median nerve) stimulation (Fig. 1, Table 1). The arcuate neurons also were observed to be influenced by activation of the vlPAG. The spontaneous neural discharge activity of the 28 neurons averaged 5.0±0.6 spikes/s. Eighteen vlPAG neurons likewise responded to P 5–6 and splanchnic nerve stimulation (Table 1).

5.2. Action of vlPAG on arcuate in EA response

Repeated splanchnic nerve stimulation every 10 min in six control animals yielded consistent arcuate responses (Fig. 1A). Bilateral microinjection of DLH (4 nM, 50 nl) into the vlPAG increased the arcuate response to splanchnic nerve stimulation in eight other cats (7±2 to 14±4 spikes/30 stim, $P<0.05$, Fig. 1B). This facilitation lasted for more than 30 min.

The EA-induced excitation of arcuate neurons was prevented by KA (1 mM, 50 nl) depolarization blockade in the vlPAG of five cats (Fig. 2B). Conversely, inadvertent injection of KA outside the vlPAG (*n*=4, Fig. 7, A 0.1–1.1) or injection of normal saline (NS) into the vlPAG did not influence EA excitation of ARC neurons during splanchnic nerve stimulation (Fig. 2A). Microinjection of DLH or KA temporarily decreased resting mean BP (4–8 mm Hg) and spontaneous firing of the arcuate neurons. Both resting BP and neuronal firing returned to their original level within 1 min. Therefore, 10 minutes later when we test the response of these neurons to splanchnic nerve stimulation, neither the resting mean BP nor the spontaneous discharge of these arcuate neurons was altered by injection of DLH or KA into the vlPAG (Tables 1 and 2).

5.3. Glutamate in arcuate-vlPAG reciprocal projections

5.3.1. Role in EA reflex inhibition—EA briefly lowered the baseline BP (<10 mm Hg) in a few animals, but for no longer than 1 to 2 min during the early phase of the 30 min of somatic nerve stimulation. However, in the later period during and following EA there were no changes in baseline BP during control (saline) or glutamatergic blockade studies. We noted no alteration of the EA-related modulation of the reflex-induced increase of BP when NS was microinjected into the arcuate or the vlPAG (Fig. 3A and C). On the other hand, this reflex inhibition was reversed by bilateral microinjection of kynurenic acid (100 nM, 50 nl) into either the arcuate or the vlPAG (Fig. 3B and D).

5.3.2. Glutamate ionotropic receptors in arcuate—We have reported previously that neurons in the vlPAG responsive to splanchnic nerve stimulation are activated by EA following administration of the vehicle, normal saline (Li et al., 2006). In the present study, we found that bilateral microinjection of the NMDA receptor antagonist, AP 5 (25 mM, 50 nl) into the arcuate nucleus of five animals did not influence the neuronal response to splanchnic nerve stimulation, but blocked EA facilitation of the splanchnic evoked response in the vlPAG (Fig. 4A). Similarly, bilateral microinjection of the glutamate non-NMDA receptor antagonist, CNQX (2 mM, 50 nl) into the arcuate of seven other cats did not influence the vlPAG neuronal response to splanchnic nerve stimulation, but completely blocked EA facilitation of the vlPAG splanchnic nerve response (Fig. 4B). Neither AP-5 nor CNQX injection in the arcuate influenced resting BP (148±4 vs. 147±4 mm Hg) or vlPAG discharge activity (5±2 vs. 4±1 spikes/s).

5.3.3. Glutamate ionotropic receptors in vlPAG—Like the arcuate, NMDA and non-NMDA receptor antagonism in the vlPAG, which did not influence resting BP or arcuate neuronal firing (Table 2), did not influence the neuronal response to splanchnic nerve stimulation, but blocked EA-induced facilitation of the arcuate neuronal response to splanchnic nerve stimulation (Fig. 4C and D). Conversely, microinjection of NS into the vlPAG did not influence the EA arcuate response (Fig. 2A). In two additional cats, accidental microinjection of the non-NMDA receptor antagonist CNQX outside the arcuate did not alter EA facilitation of the arcuate neural response to splanchnic nerve input (Fig. 7 top panel, ARC).

5.4. Role of acetylcholine in arcuate and vlPAG

Microinjection of ACh into the arcuate nucleus transiently reduced (30–60 s) resting MBP by 5±1 mm Hg ($P<0.05$). Baseline BP had recovered by the time we applied BK to the gallbladder 10 min later, (Fig. 5A). The BK-induced reflex increase in BP was decreased by ACh from 39±6 to 23±9 mm Hg for 20 min ($P<0.05$) (Fig. 5A). Furthermore, microinjection of atropine into the arcuate rapidly reversed EA inhibition of the BK-induced increase in BP ($P<0.05$) (Fig. 5B). This reversal contrasts with the prolonged inhibition of reflex response

by EA following administration of the vehicle into the arcuate nucleus (Fig. 3A). Microinjection of ACh into the vlPAG did not change resting MBP.

In another group of animals, microinjection of ACh into the arcuate nucleus did not change resting discharge activity of vlPAG neurons (2 ±1 vs. 3±1 spikes/s, $P>0.05$) but did increase the splanchnic nerve-evoked vlPAG response ($n=8$, $P<0.05$), an effect that lasted for 10 min (Fig. 6A). Conversely, microinjection of atropine into the arcuate, which likewise did not influence resting activity of vlPAG neurons (2±1 vs.4 ±1 spikes/s, $P>0.05$), blocked the EA-induced facilitation of the vlPAG response (Fig. 6B). In contrast to the evident role of cholinergic receptors in the arcuate, ACh in the vlPAG did not change either the resting discharge of arcuate neurons (Table 2) or the arcuate response to splanchnic nerve stimulation (Fig. 6C). Furthermore, atropine in the vlPAG did not significantly influence the spontaneous activity of arcuate neurons (Table 2) or the EA-related facilitation of the arcuate response (Fig. 6D).

5.5. Anatomical verification of injection sites

All injections and recordings were verified to be in the arcuate nucleus or the vlPAG, according to the atlas of Fikova and Marsala (1967) (Fig. 7).

5.6. Arcuate-vlPAG projections

In three rats, we observed that the microsphere tracer deposited in the vlPAG was transported in a retrograde fashion both rostrally and caudally throughout the arcuate nucleus. Similarly, microspheres injected into the arcuate of four other rats, were observed to be present throughout the vlPAG at multiple rostral–caudal levels. Fig. 8 demonstrates high and low power confocal images of neurons labeled with microspheres in the arcuate and vlPAG of a rat when the retrograde tracers were injected into the opposite nucleus (Fig. 9).

6. Discussion

Our previous studies have documented that the arcuate nucleus provides excitatory projections to the vlPAG and serves as an important relay station from the arcuate to the rVLM (Li et al., 2006, 2008, 2009; Tjen-A-Looi et al., 2003, 2006). The present study extends these observations by providing evidence for reciprocal projections between the arcuate and the vlPAG that participate in the EA-cardiovascular response. More specifically we found that excitation of vlPAG neurons enhances the arcuate response to splanchnic stimulation, while blockade of vlPAG neurons with KA limits excitation of arcuate neurons by EA. These observations indicate that EA-induced excitation of arcuate neurons requires input from the vlPAG. This interaction is an extension of our previous observation that excitability of vlPAG neurons during EA is dependent on input from the arcuate nucleus (Li et al., 2006, 2008, 2009). Thus, in the present study we provide the first evidence for a functional reciprocal excitatory connection between these two nuclei. Importantly, we also found that, following activation of the arcuate by 30 min of EA, neurons in this region and in the vlPAG continue to discharge for more than 60 min after termination of EA, in part, due to activation of this reciprocal ARC-vlPAG circuit (Fig. 2A) (Li et al., 2006). This interactive network thus provides a mechanism underlying the long-lasting effect of EA, in addition to the opioid and GABA-mediated inhibition in the rVLM, which can last from 30 min to 1 h following termination of EA (Tjen-A-Looi et al., 2007).

The present study used rats to demonstrate anatomically bidirectional projections between the arcuate nucleus and the vlPAG, while cats were used for our functional studies. Our laboratory has shown previously that the anatomical circuitry participating in the EA-related

cardiovascular inhibitory response in rats and cats is identical (Li et al. 2009; Moazzami et al., 2010). Furthermore, Adams (1979) has described that brain mechanisms involved in aggression in primitive mammals and in primates are similar to those in rats and cats. In fact, there are more similarities than differences between these species. We, therefore, believe that our data obtained in rats with respect to the reciprocal projections between arcuate and vlPAG also apply to cats.

Both arcuate and vlPAG neurons receive convergent somatic and visceral afferent input from the median nerve (P 5–6, activated during EA stimulation) and the splanchnic nerve stimulated during visceral reflex-induced sympathoexcitation. In the present study we recorded discharge activity after the cats had been stabilized for 1 to 2 h following surgery, resulting in higher resting firing rate than we had observed previously (1±1 vs. 5±1 spikes/s, previous vs. current study).

The current study also documented for the first time that reciprocal excitatory projections between the arcuate nucleus and the vlPAG that participate in the EA-cardiovascular response are glutamatergic in nature since microinjection of the glutamate receptor antagonist, kynurenic acid, into the arcuate nucleus reversed the reflex pressor response induced by application of BK to the gallbladder. Moreover, microinjection of the NMDA or non-NMDA receptor antagonists, AP5 or CNQX, blocked the reciprocal excitation between the arcuate and the vlPAG. Thus, glutamate through its action on ionotropic receptors is essential to the reciprocal reinforcement between the midbrain and the ventral hypothalamus that serves to prolong the influence of EA on cardiovascular function.

NMDA and non-NMDA ionotropic receptors have been shown to function differently in different nuclei. For instance, Manuel et al. and Bodnár et al. have reported that non-NMDA and NMDA receptors in the cortex (Manuel et al., 1995) and in the paraventricular nucleus (Bodnár et al., 2005) function differently. In contrast, Gee et al. (2002) have shown that both spinal NMDA and non-NMDA receptors are similarly involved in the pressor reflex response to abdominal ischemia. In addition, Zhou et al. (2006) have reported that the excitatory cardiovascular reflex response requires medullary transmission through glutamatergic neurons that rely on activation of both NMDA and non-MNDA receptors. Our present results show that both non-NMDA and NMDA receptors are involved in a similar fashion in the arcuate nucleus, suggesting that both the non-NMDA and NMDA receptors are important in this region of the hypothalamus.

We have reported that more neurons in the caudal than in the rostral vlPAG are related to EA inhibition of the rVLM neurons (Guo et al., 2004; Li et al., 2009). However, we have shown that many neurons in the rostral vlPAG are activated by EA and that a portion of the arcuate-rVLM pathway courses through this region (Li et al., 2009). Thus, in the present study, injections of glutamate agonists and antagonists were performed in the rostral vlPAG since this region is much more readily accessed for recordings and microinjections because it is not protected by the bony tentorium. Most importantly, the results of the current study demonstrate that the rostral vlPAG also plays a role in the EA-cardiovascular inhibition and provides reciprocal projections between the arcuate nucleus and vlPAG. We conclude therefore that, while the caudal vlPAG is an important region in the long-loop arcuate-rVLM pathway for the EA-cardiovascular response, the rostral vlPAG is important in the reciprocal arcuate-vlPAG pathway that helps to prolong EA-cardiovascular modulation.

Using the technique of microdialysis, we recently demonstrated that the concentration of GABA, but not glutamate, is altered by EA in dialysates collected from the extracellular space in the vlPAG (Fu and Longhurst, 2009). Although the present study documented an important role for glutamate in this region of the midbrain, and may seem to be at odds with

our recent publication, there are a number of differences between the two investigations. First, the extracellular concentration of glutamate as measured previously is a function of release from both neuronal and non-neuronal cellular elements, whereas the present study investigated the role of glutamate only with respect to vlPAG neuronal activity. Second, extracellular concentrations reflect the release of glutamate from a population of neurons (and glial cells) as well as uptake and metabolism of the released neurotransmitter outside the synaptic region (Baker et al., 2002). Thus, it is possible that a rapid uptake of released glutamate or a small increase in glutamate in the vlPAG could not be detected by microdialysis in the previous study (Zhou et al. 2006, 2007). Electrophysiological recordings as performed in the present study primarily focus on glutamate release and its action on ionotropic receptors in the synaptic cleft. With respect to this last consideration, the group of neurons involved in the EA-cardiovascular response may constitute only a fraction of the overall cell population in the vlPAG. Thus, despite the differences in observations between our earlier and the current study, with respect to the role of glutamate in the vlPAG, we believe that it is difficult to compare directly the results, given the different techniques employed in the two studies. From data in the current study, we conclude that, in the population of cells that take part in processing the interaction between somatic and visceral afferents in the vlPAG as well as interactions between the arcuate and the vlPAG, glutamate's action on its ionotropic receptors is important in the EA-cardiovascular response.

Meister et al. (2006) reported that some neurons in the arcuate nucleus contain choline acetyltransferase (ChAT) as well as the vesicular acetylcholine transporter. They suggested that ACh, along with other peptides derived from these neurons, has functional significance. It has been shown that ACh causes excitation of neurons in many nuclei including the rVLM and arcuate nucleus (Zhu et al., 1990; Lin and Li, 1990; Nakamura et al., 2009) and therefore can increase baseline blood pressure. However, likewise there are a number of studies indicating that the arcuate nucleus is a depressor nucleus (Sitsen et al., 1982; Mastrinni et al., 1989), which inhibits reflex-induced increases in BP (Li et al., 2006, 2009). The current study demonstrates that excitation of neurons with ACh in the arcuate reduces the sympathoexcitatory cardiovascular reflex response and causes a small transient decrease of the baseline blood pressure. Furthermore, the present study demonstrates that exogenous ACh applied to the arcuate facilitates the vlPAG neural response to splanchnic nerve stimulation, while muscarinic blockade with atropine in the arcuate blocks EA facilitation of vlPAG neurons. Therefore, it does appear that in addition to glutamate, ACh in the arcuate nucleus participates in EA modulation of sympathoexcitatory cardiovascular reflexes. The possibility of an interaction between ACh and glutamate will require further investigation. On the other hand, ACh injected into the vlPAG did not excite arcuate neurons and atropine in this region did not block EA excitation of arcuate neurons. Thus, neither atropine nor ACh influenced baseline BP in our investigation suggesting that cholinergic receptor stimulation in this midbrain region is not responsible for tonic outflow that regulates cardiovascular function.

The long-lasting cardiovascular inhibitory effect of EA has been shown to last between 10 and 12 h, depending on the model employed (Guo et al., 1981; Lin and Li, 1981; Lovick et al., 1995; Yao et al., 1982). Prolonged release and the sustained action of inhibitory neurotransmitters in the rVLM (Tjen-A-Looi et al., 2007) as well as the reciprocal neuronal circuit between the arcuate and the vlPAG, as shown in this paper, appear to perpetuate the response, and thus explain at least part of this long-term modulation. However, other mechanisms may be evoked to induce the very prolonged inhibition of blood pressure that can last for weeks in patients with mild to moderate hypertension (Li and Longhurst, 2007). In this regard, Guo et al. (1996) and He et al., (1995) have reported that acupuncture increases the mRNA expression of opioid precursors in the brain. Data from our laboratory

using real time PCR recently have shown that preproenkephalin is increased after completion of a single 30 min application of EA at P 5–6 in rats (Li et al., 2010). The roles of mRNA expression of opioid and other neurotransmitter precursors, and the neurotransmitters released from hypothalamus and the midbrain that have been identified in the current investigation are worthy of further investigation.

7. Conclusion

Reciprocal excitatory projections exist between the arcuate nucleus and midbrain vlPAG that participate in EA inhibition of cardiovascular function. Glutamatergic and to a lesser extent cholinergic mechanisms underlie activation of these neuronal circuits. The reinforcement that results from activation of this reciprocal innervation appears to be one of the mechanisms by which EA exerts long-lasting inhibition of sympathoexcitatory reflex elevations of blood pressure.

Acknowledgments

We gratefully acknowledge Mr. Cao YX, Department of Physiology, Shanghai Medical College of Fudan University, China for the development of the four-channel data acquisition system and the software for analyzing the data. We also like to thank Rainier Cabatbat, Alvin D. Nguyen, Ryan Perry, and Joshua Liu for their technical assistance. This work was supported by National, Heart, Lung and Blood Institute Grants HL-72125 and HL-63313 and the Larry K. Dodge and Susan Samueli Endowed Chairs (J.C. Longhurst).

References

Adams, DB. The Behavioral and Brain Sciences V.2 Brain Mechanisms for Offense, Defense and Submission. Cambridge University Press; 1979.

Baker D, Xi Z, Shen H, Swanson C, Kalivas P. The origin and neuronal function of in vivo nonsynaptic glutamate. J Neurosci. 2002; 22:9134–9141. [PubMed: 12388621]

Bodnár I, Bánky Z, Nagy G, Halász B. Non-NMDA glutamate receptor antagonist injected into the hypothalamic paraventricular nucleus blocks the suckling stimulus-induced release of prolactin. Brain Res Bull. 2005; 65:163–168. [PubMed: 15763183]

Fikova, E.; Marsala, J. Stereotaxic atlases for the cat, rabbit, and rat. In: Bures, J.; Petran, M.; Zachar, J., editors. Electrophysiological Methods in Biological Research. Academia Publishing House of the Czechoslavak Academy of Sciences; 1967. p. 653-731.

Fu L, Longhurst C. Electroacupuncture modulates vlPAG release of GABA through presynaptic cannabinoid CB1 receptor. J Appl Physiol. 2009; 106:1800–1809. [PubMed: 19359606]

Gee S, Tjen-A-Looi S, Hill J, Chahal P, Longhurst J. Role of spinal NMDA and non-NMDA receptors in the pressor reflex response to abdominal ischemia. Am J Physiol. 2002; 282:R850–R857.

Guo XQ, Jai RJ, Cao QY, Guo ZD, Li P. Inhibitory effect of somatic nerve afferent impulses on the extrasystole induced by hypothalamic stimulation. Acta Physiol Sin. 1981; 33:343–350.

Guo HF, Wang XM, Tian JH, Huo YP, Han JS. Brain substrates activated by electroacupuncture (EA) of different frequencies (II): role of Fos/Jun proteins in EA induced transcription of preproendephalin and preprodynorphin genes. Brain Res Mol Brain Res. 1996; 43:167–173. [PubMed: 9037530]

Guo ZL, Moazzami A, Longhurst J. Electroacupuncture induces c-Fos expression in the rostral ventrolateral medulla and periaqueductal gray in cats: relation to opioid containing neurons. Brain Res. 2004; 1030:103–115. [PubMed: 15567342]

He LF, Yu Y, Gao M. Temporal alteration of proopiomelanocortin mRNA level in rat hypothalamic arcuate nucleus following electroacupucnture. World J Acup-Mox. 1995; 5:36–41.

Li P, Longhurst JC. Long-lasting inhibitory effect of EA on blood pressure in patients with mild to moderate hypertension. Soc Neurosci. 2007:35. (abstract).

Li P, Pitsillides K, Rendig S, Pan HL, Longhurst J. Reversal of reflex-induced myocardial ischemia by median nerve stimulation: a feline model of electro-acupuncture. Circulation. 1998; 97:1186–1194. [PubMed: 9537345]

Li P, Tjen-A-Looi S, Longhurst J. Rostral ventrolateral medullary opioid receptor subtypes in the inhibitory effect of electroacupuncture on reflex autonomic response in cats. Auton Neurosci Basic and Clinical. 2001; 89:38–47.

Li P, Tjen-A-Looi S, Longhurst J. Excitatory projections from arcuate nucleus to ventrolateral periaqueductal gray in electroacupuncture inhibition of cardiovascular reflexes. Am J Physiol. 2006; 209:H2535–H2542.

Li P, Tjen-A-Looi S, Guo Z, Longhurst JC. Reciprocal neuronal projections between arcuate and ventrolateral periaqueductal gray participate in long-lasting EA inhibition of reflex blood pressure elevation. FASEB J. 2008:22.

Li P, Tjen-A-Looi S, Guo Z, Fu LW, Longhurst JC. Long-loop pathways in cardiovascular electroacupuncture responses. J Appl Physiol. 2009; 106:620–630. [PubMed: 19074569]

Li M, Tjen-A-Looi SC, Longhurst JC. Electroacupuncture enhances preproenkephalin mRNA expression in rostral ventrolateral medulla of rats. Neurosci Lett. 2010; 477:61–65. [PubMed: 20399834]

Lin SX, Li P. Mechanism of inhibitory effect of electro-acupuncture on noradrenaline hypertension. Acta Physiol Sin. 1981; 33:335–342.

Lin Q, Li P. Rostral medullary cholinergic mechanisms and chronic stress-induced hypertension. J Auton Nerv Syst. 1990; 31:211–217. [PubMed: 2084185]

Lovick TA, Li P, Schenberg LC. Modulation of the cardiovascular defence response by low frequency stimulation of a deep somatic nerve in rats. J Auton Nerv Syst. 1995; 50:347–354. [PubMed: 7714329]

Manuel A, Castro-Alamancos, Jose Borrell. Contribution of NMDA and non NMDA glutamate receptors to synchronized excitation and cortical output in the primary motor cortex of the rat. Brain Res Bull. 1995; 37:539–543. [PubMed: 7633903]

Mastrinni J, Palkovits M, Kunos G. Activation of brainstem endorphinergic neurons causes cardiovascular depression and facilitates baroreflex bradycardia. Neuroscience. 1989; 33:559–566. [PubMed: 2636709]

Meister B, Gomuc B, Suarez E, et al. Hypothalamic proopiomelanocortin (POMC) neurons have a cholinergic phenotype. Eur J Neurosci. 2006; 24:2731–2740. [PubMed: 17156199]

Moazzami A, Tjen-A-Looi SC, Guo Z, Longhurst JC. Serotonergic projection from nucleus raphe pallidus to rostral ventrolateral medulla modulates cardiovascular reflex responses during acupuncture. J Appl Physiol. 2010; 108:1336–1346. [PubMed: 20133441]

Nakamura T, Bhatt S, Sapru HN. Cardiovascular responses to hypothalamic arcuate nucleus stimulation in the rat: role of sympathetic and vagal efferents. Hypertension. 2009; 54:1369–1375. [PubMed: 19884562]

Paxinos, G.; Watson, C. The Rat Brain in Stereotaxic Coordinates. Academic Press; 2005.

Sitsen J, Ven Ree J, De Jong W. Cardiovascular and respiratory effects of beta-endorphin in anesthetized and conscious rats. J Cardiovasc Pharmacol. 1982; 4:883–888. [PubMed: 6185778]

Tam KC, Yiu HH. The effect of acupuncture on essential hypertension. Am J Chin Med. 1975; 3:369–375. [PubMed: 1202935]

Tjen-A-Looi SC, Li P, Longhurst JC. Prolonged inhibition of rostral ventral lateral medullary premotor sympathetic neuron by electroacupuncture in cats. Auton Neurosci Basic and Clinical. 2003; 106 (2):119–131.

Tjen-A-Looi SC, Li P, Longhurst JC. Midbrain vIPAG inhibits rVLM cardiovascular sympathoexcitatory responses during acupuncture. Am J Physiol. 2006; 209:H2543–H2553.

Tjen-A-Looi SC, Li P, Longhurst JC. Role of medullary GABA, opioids, and nociceptin in prolonged inhibition of cardiovascular sympathoexcitatory reflexes during electroacupuncture in cats. Am J Physiol Heart Circ Physiol. 2007; 293:H3627–H3635. [PubMed: 17890425]

Yao T, Andersson S, Thoren P. Long-lasting cardiovascular depression induced by acupuncture-like stimulation of the sciatic nerve in unanaesthetized spontaneously hypertensive rats. Brain Res. 1982; 240:77–85. [PubMed: 7201339]

Zhang CL. Clinical investigation of acupuncture therapy. Clin J Med. 1956; 42:514–517.

Zhou W, Fu LW, Tjen-A Looi SC, Guo ZL, Longhurst JC. Role of glutamate in a visceral sympathoexcitatory reflex in rostral ventrolateral medulla of cats. Am J Physiol Heart Circ Physiol. 2006; 291:H1309–H1318. [PubMed: 16632546]

Zhou W, Fu LW, Guo Z, Longhurst J. Role of glutamate in rostral ventrolateral medulla in acupuncture-related modulation of visceral reflex sympathoexcitation. Am J Physiol Heart Circ Physiol. 2007; 292:H1868–H1875. [PubMed: 17158649]

Zhu DN, Guo XQ, Li P. Relationship between the rostral medullary cholinergic mechanism and the cardiovascular component of the defence reaction. Chin J Physiol. 1990; 6:86–94.

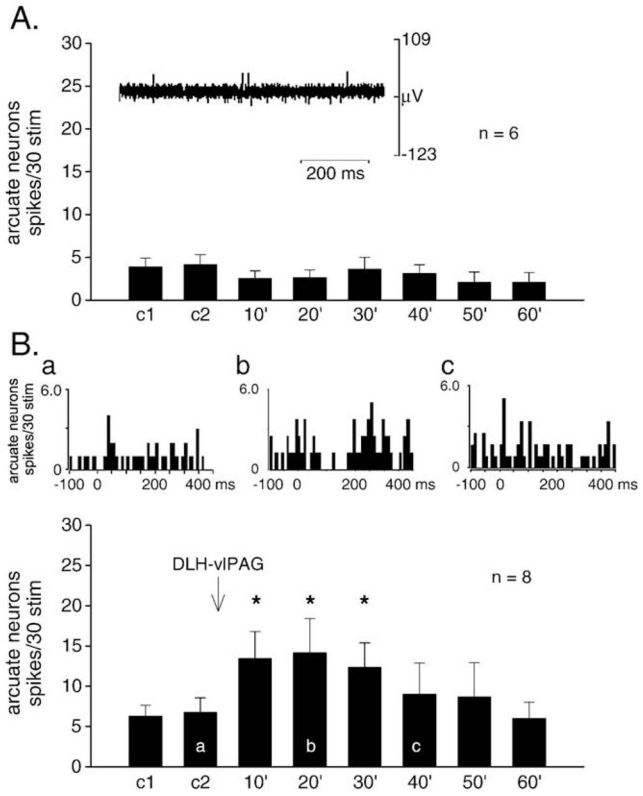

Fig. 1.

Panel A. Histogram to show repeated splanchnic nerve stimulation at 10 min intervals evoked consistent arcuate responses. An original neuronal recording is inserted on the top. Panel B. histogram shows group responses documenting facilitation of arcuate neuronal response by bilateral microinjection of dl-homocysteic acid (DLH, 4 nM, 50 nl) into vlPAG. Facilitation lasted for more than 30 min. **P*<0.05 compared to controls (c1, c2). Peristimulus histograms on the top of this panel show evoked responses to splanchnic nerve stimulation that was increased after injection of DLH into the vlPAG. The letters a, b and c represent times of recordings in the bar histogram.

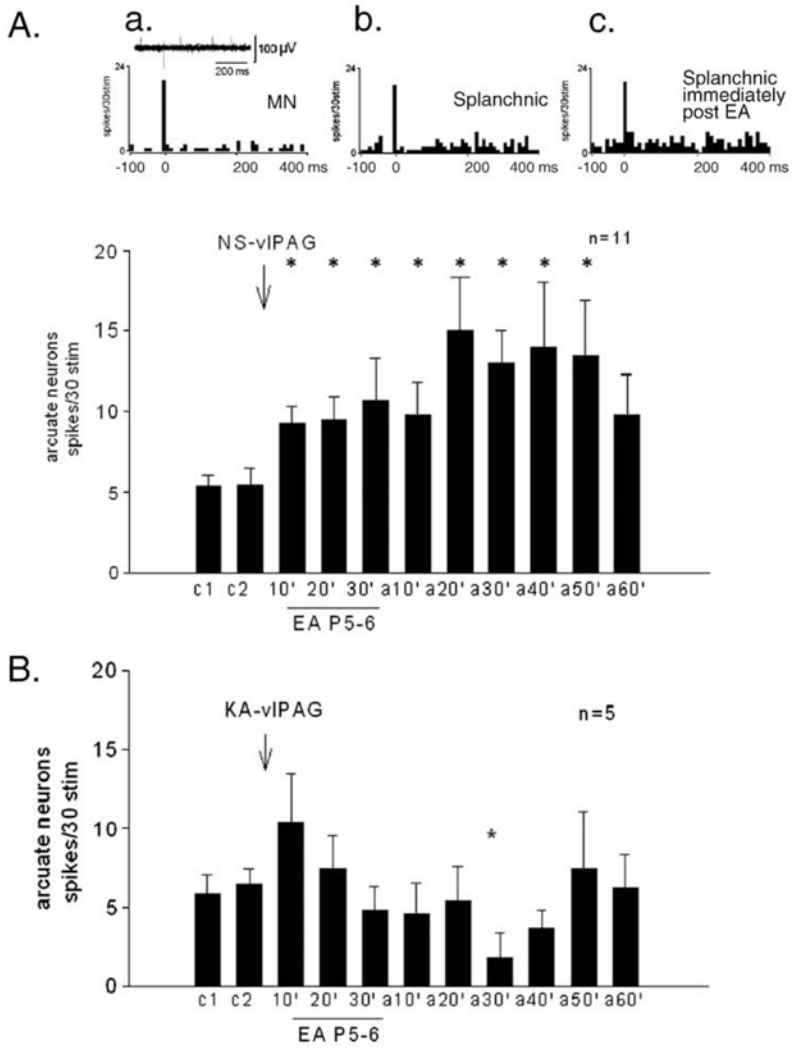

Fig. 2.

EA increased the arcuate response to splanchnic nerve stimulation for more than 60 min (Panel A). Inset for panel a represents a peristimulus histograms of the evoked activity during bilateral stimulation of median nerve at P 5–6 acupoints (3 mV, 2 Hz, 30 stimuli). An original recording is inserted on the top. Panel b displays response of splanchnic nerve stimulation (2 mV, 2 Hz, 30 stimuli) before EA. Panel c, response of the splanchnic nerve stimulation after 30 min EA shows facilitation of the arcuate neuronal response to splanchnic nerve stimulation. The stimulation artifact is shown on the *x*-axis at 0 ms. Panel B. arcuate responses following bilateral microinjection of kainic acid (KA, 1 mM, 50 nl) into the vlPAG, which blocked EA-induced facilitation of the arcuate neural response. **P*<0.05 compared to controls; NS is normal saline; splanchnic nerve stimulation was applied every 10 min. Letters below bar: c=control, a=after EA.

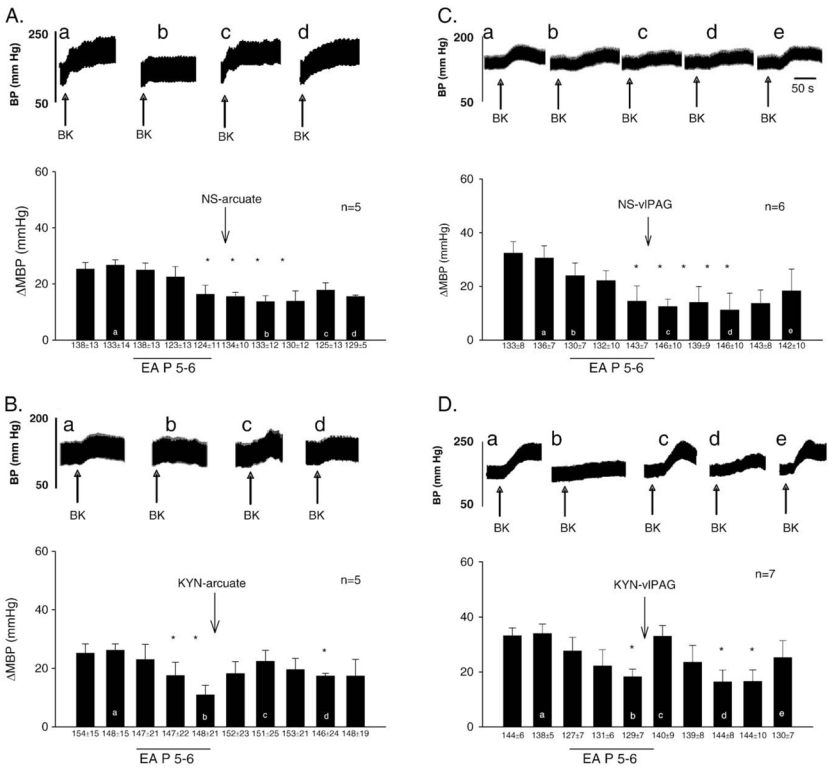

Fig. 3.

Bilateral microinjection of the glutamate receptor antagonist, kynurenic acid (KYN, 50–100 nM, 50 nl), into the arcuate nucleus blocked EA inhibition of the excitatory reflex response induced by application of BK to the gallbladder (Panel B), while microinjection of NS into the arcuate did not influence the EA-related inhibition (Panel A). Microinjection of KYN into vlPAG also blocked EA modulation of the reflex increase of BP (Panel D), while injection of NS into the vlPAG did not alter the EA response (Panel C). In each panel, the upper figures are original BP recordings that correspond with the letters a, b, c and d shown in the bar histogram. These results indicate that EA inhibition of the reflex pressor response is related to activation of glutamate receptors in the arcuate nucleus. **P*<0.05 compared to controls. Means±SEM below each bar histogram displays baseline mean blood pressure (MBP).

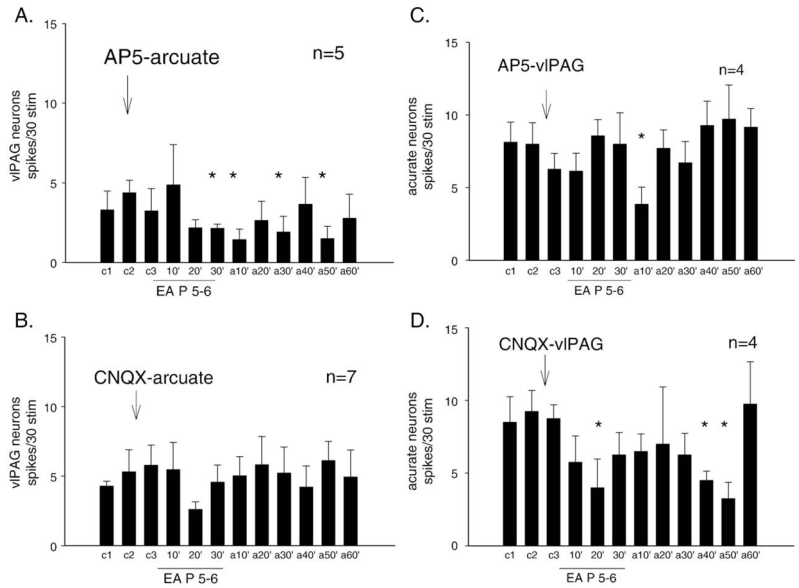

Fig. 4.

EA did not induce excitation but rather inhibited the vlPAG neural response to splanchnic nerve stimulation (applied every 10 min) after injection of the glutamate ionotropic receptor antagonists, AP-5 (Panel A) and CNQX (Panel B), in the arcuate nucleus. Likewise, after injection of AP-5 (Panel C) and CNQX (Panel D) in the vlPAG, EA did not facilitate arcuate neural response to splanchnic nerve stimulation (every 10 min). **P*<0.05 compared to controls.

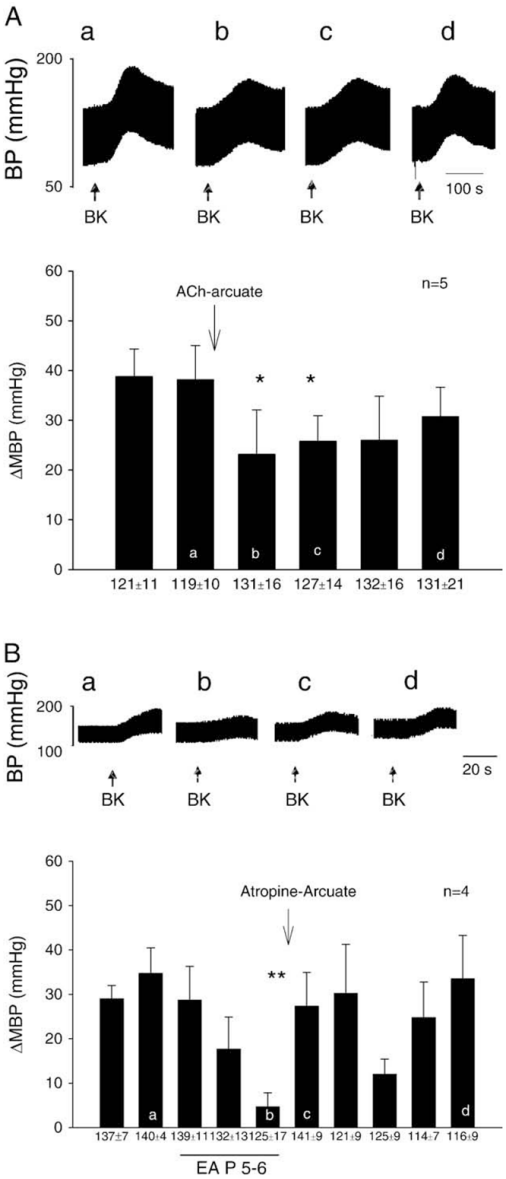

Fig. 5.

Panel A. Microinjection of ACh into the arcuate bilaterally reduced the BK induced reflex increase of BP. Upper panel shows the original recording of BP response to BK applied to gallbladder. Lower panel shows the bar histogram of the BP response to BK application to gallbladder. Panel B. Bilateral microinjection of atropine into arcuate rapidly reversed EA inhibition of the reflex increase of BP induced by application of BK to the gallbladder. Upper panel displays the original recordings of BP response to BK applied to gallbladder. Lower panel shows the bar histogram of the BP response to BK application to gallbladder. The letters a, b, c and d correspond with individual examples of blood pressure tracings. These results indicate that EA inhibition of the reflex pressor response is related to activation of cholinergic receptors in the arcuate nucleus. **P*<0.05 compared to controls. Means±SEM below each bar histogram display baseline mean blood pressure (MBP).

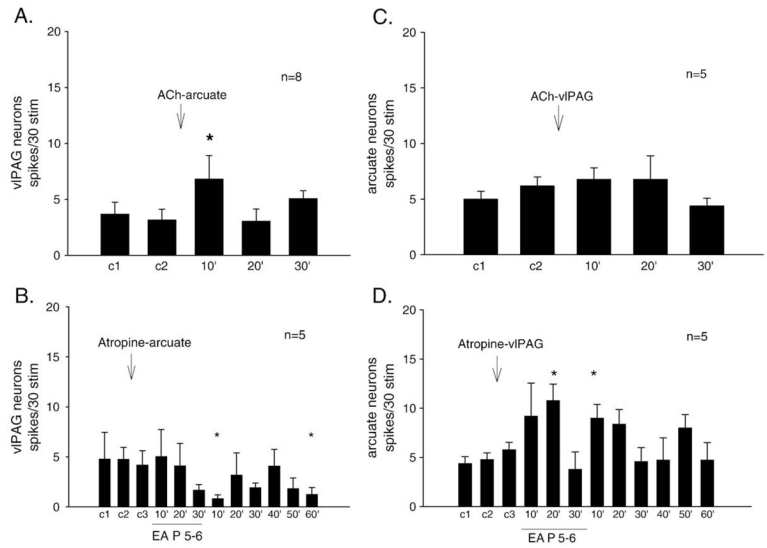

Fig. 6.

Panel A: Microinjection of ACh into the arcuate nucleus enhanced the vlPAG neuronal response to splanchnic nerve stimulation. Panel B: Microinjection of the muscarinic receptor antagonist, atropine, into the arcuate blocked EA excitation of the vlPAG neural response. Panel C: Microinjection of ACh into the vlPAG did not influence the arcuate neural response to splanchnic nerve stimulation. Panel D: Microinjection of atropine into the vlPAG did not alter EA excitation of the arcuate neural response. **P*<0.05 compared to controls.

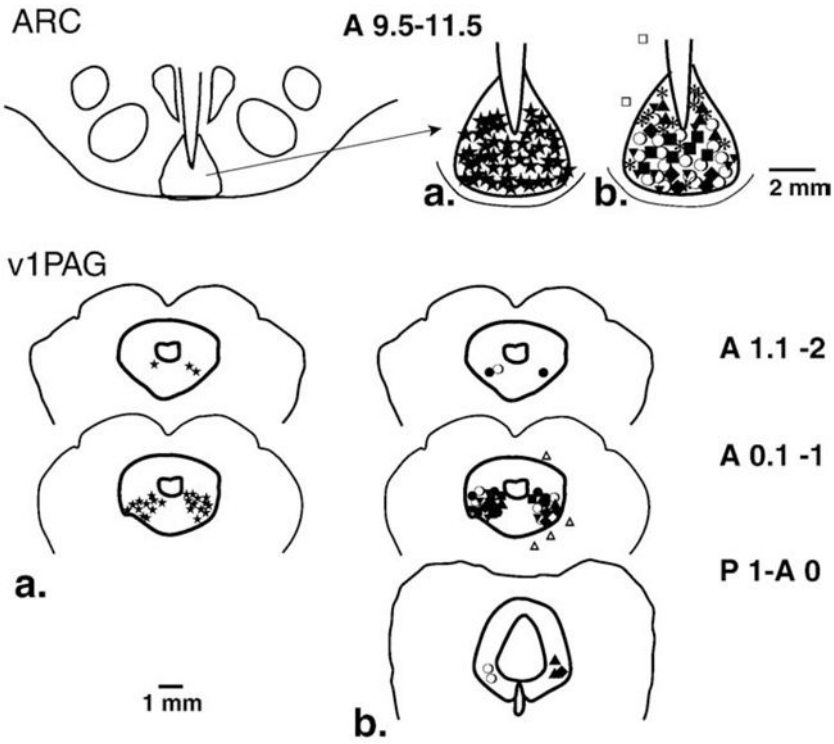

Fig. 7.

Composite map of brain sections showing locations of microinjection and recording sites in the arcuate nucleus and vlPAG. For simplicity, all microinjection sites have been placed on one side. Abbreviations: (○) NS in ARC/vlPAG (*n*=19/8); (●) DLH in vlPAG (*n*=8); (◇) KYN in arcuate/vlPAG (*n*=5/7); (▲) KA in vlPAG (*n*=5); (△) KA outside vlPAG (*n*=4); (■) CNQX in ARC/vlPAG (*n*=7/4); (□) CNQX outside ARC/vlPAG (*n*=2); (◆) AP5 in ARC/vlPAG (*n*=5/7); (*) ACh in ARC/vlPAG (*n*=13/5); (▼) atropine in ARC/vlPAG (*n*=9/5); (★) neuronal recording in ARC/vlPAG (*n*=50/25).

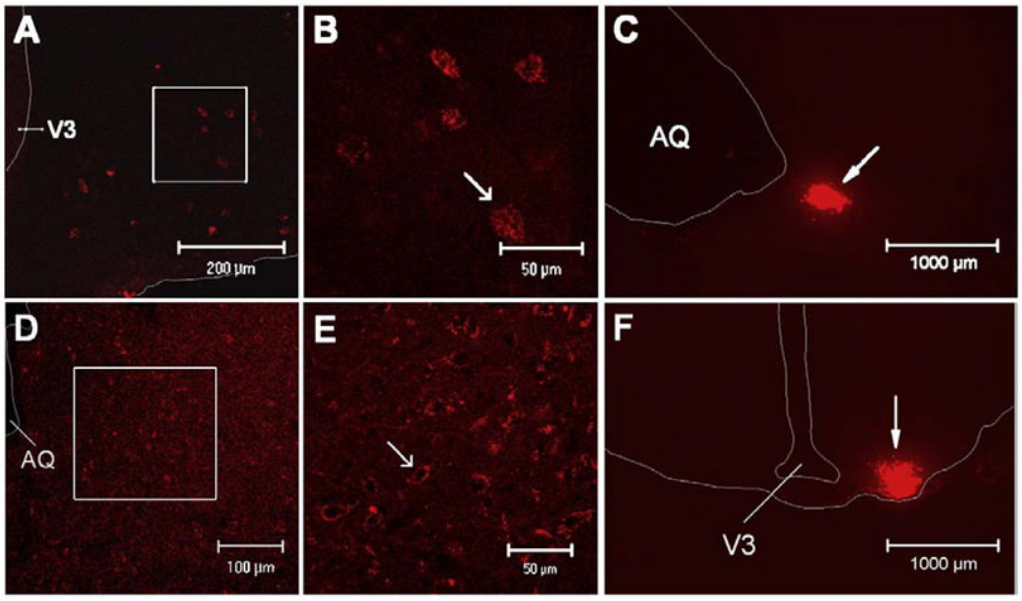

Fig. 8.

Confocal microscopic images showing neurons labeled with a retrograde microsphere tracer in arcuate nucleus (A and B; Bregma −2.04) and vlPAG (D and E; Bregma −7.92) of rats. Panels C and F show microinjection sites of the retrograde tracer in vlPAG (*C*, Bregma −8.52) and the arcuate nucleus (*F*, Bregma −2.16), respectively. A and D: low power photomicrographs; B and E: magnified regions shown within boxes in A and D. Arrows in Panels B and E indicate neurons containing retrograde tracer. Scale bars in panels A, D, B and E, and C and F represent 200, 100, 50 and 1000 μm, respectively. Arrows in the Panels C and F indicate injection sites. AQ, aqueduct; V3, third ventricle.

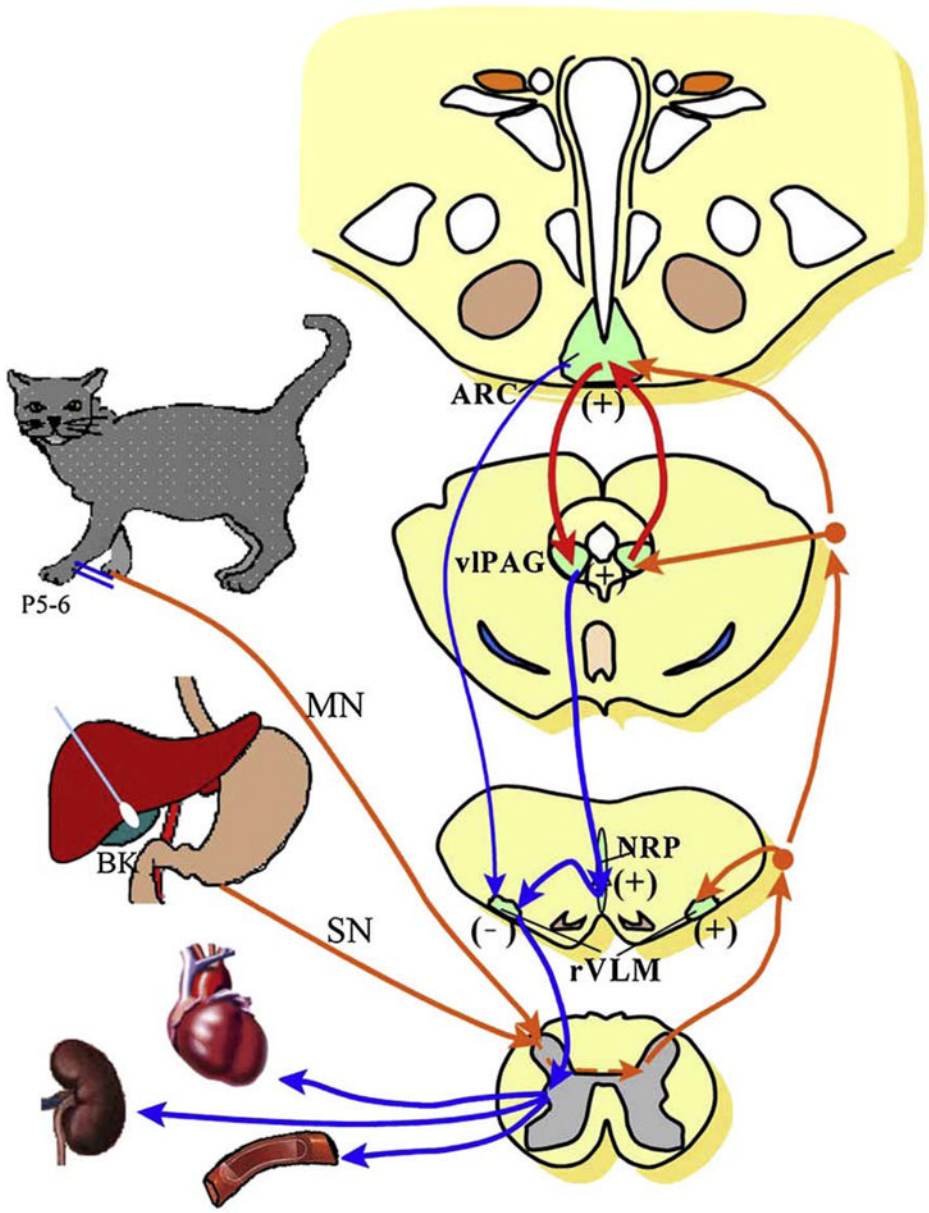

Fig. 9.

Neuronal pathways and mechanisms underlying the effect of acupuncture on a visceral sympathoexcitatory reflex. Our previous studies have demonstrated that stimulation of both cardiovascular acupoints P 5–6 (overlying the median nerve) and gallbladder activating afferents in the splanchnic nerve (SN) lead to activation of premotor neurons in the rostral ventrolateral medulla (rVLM). The rVLM provides output to the intermediolateral column of the spinal cord, where sympathetic motoneurons project to the heart and vascular system. Thirty minutes of EA at P 5–6 activates a long-loop pathway located in the hypothalamic arcuate nucleus (ARC), the midbrain ventrolateral periaqueductal gray (vlPAG), and the medullary nucleus raphe pallidus (NRP) that in turn inhibits the rVLM. The present study shows that 30 min EA activates the arcuate-vlPAG reciprocal circuit, which contributes to the EA long-lasting effect. Orange arrows, →, indicate afferent input from the SN and P 5–6 acupoints (MN); red arrows, →, indicate reciprocal excitatory projections between the

arcuate and vlPAG, blue arrows; →, indicate efferent projections from the arcuate, vlPAG, NRP and rVLM to the spinal cord, heart, blood vessels and kidney. (For interpretation of the references to colour in this figure legend, the reader is referred to the web version of this article.)

Table 1

Characteristics of arcuate and vlPAG neurons.

Location of neurons	No. of neurons	Spontaneous activity (spikes/s)	Response to P 5–6 stimulation (spikes/30 st)	Response to splanchnic nerve stimulation (spikes/30 stim)
Arcuate	28	5.0±0.6	9.8±0.9	6.3±0.4
vlPAG	18	3.3±1.2	18.6±4.4	4.8±0.8
P value		NS	NS	NS

NS, there is no significant difference in comparing arcuate and vlPAG data.

Table 2

Resting BP and neural activity 5 min after vlPAG microinjection.

Location of neurons	**injection**	**DLH vlPAG *n*=8**	**KA vlPAG *n*=5**	**AP-5 vlPAG *n*=4**	**CNQX vlPAG *n*=7**	**ACh vlPAG *n*=5**	**Atropine vlPAG *n*=5**
Resting MBP (mm Hg)	Pre	130±26	123±11	141±8	152±5	144±7	116±12
	Post	128±23	124±13	146±8	147±4	139±7	110±8
Arcuate neurons (spikes/s)	Pre	3±1	4±1	5±1	5±2	8±2	7±2
	Post	4±1	2±1	8±2	4±1	7±2	5±1
P value	Pre vs. post	NS	NS	NS	NS	NS	NS

NS, no significant difference in comparing the pre and post-injection data of resting MBP and arcuate neurons firing.